0026-895X/09/7601-25–37$20.00
MOLECULAR PHARMACOLOGY
Copyright © 2009 The American Society for Pharmacology and Experimental Therapeutics
Mol Pharmacol 76:25–37, 2009

Vol. 76, No. 1
55384/3481205
Printed in U.S.A.

Contribution of Binding Enthalpy and Entropy to Affinity of Antagonist and Agonist Binding at Human and Guinea Pig Histamine H_1-Receptor

Hans-Joachim Wittmann, Roland Seifert, and Andrea Strasser

Faculty of Chemistry and Pharmacy (H.-J.W.) and Department of Pharmaceutical/Medicinal Chemistry I, School of Pharmacy (A.S.), University of Regensburg, Regensburg, Germany; and Institute of Pharmacology, Medical School of Hannover, Hannover, Germany (R.S.)

Received February 9, 2009; accepted April 3, 2009

ABSTRACT

For several GPCRs, discrimination between agonism and antagonism is possible on the basis of thermodynamics parameters, such as binding enthalpy and entropy. In this study, we analyze whether agonists and antagonists can also be discriminated thermodynamically at the histamine H_1 receptor (H_1R). Because previous studies revealed species differences in pharmacology between human H_1R (hH_1R) and guinea pig H_1R (gpH_1R), we analyzed a broad spectrum of H_1R antagonists and agonists at hH_1R and gpH_1R. [^{3}H]Mepyramine competition binding assay were performed at five different temperatures in a range from 283.15 to 303.15 K. In addition, we performed a temperature-dependent three-dimensional quantitative structure activity relationship study to predict binding enthalpy and entropy for histaprodifen derivatives, which can bind to H_1R in two different orientations. Our studies revealed significant species differences in binding enthalpy and entropy between hH_1R and gpH_1R for some antagonists and agonists. Furthermore, in some cases, we found changes in heat capacity of the binding process that were different from zero. Differences in flexibility of the ligands may be responsible for this observation. For most ligands, the binding process to hH_1R and gpH_1R is clearly entropy-driven. In contrast, for the endogenous ligand histamine, the binding process is significantly enthalpy-driven at both species isoforms. Thus, a definite discrimination between antagonism and agonism based on thermodynamic parameters is possible for neither hH_1R nor gpH_1R, but thermodynamic analysis of ligand-binding may be a novel approach to dissect agonist- and antagonist-specific receptor conformations.

The histamine H_1-receptor (H_1R) is a biogenic amine receptor that belongs to the G-protein-coupled receptors (GPCRs) and couples to G_q-proteins (Hill et al., 1997). H_1R antagonists (Fig. 1, **1**-**8**) have relevance in treatment of allergic diseases. In contrast, H_1R agonists (Fig. 1, **9**-**22**) are used as tools to study the pharmacology and functionality of the H_1R on a molecular level. Several classes of synthetic H_1R agonists are known, including phenylhistamines (Leschke et al., 1995; Zingel et al., 1995), histaprodifens (Elz et al., 2000; Menghin et al., 2003), and phenoprodifens (Strasser et al., 2008b).

Weiland et al. (1979) were the first to find that antagonists and agonists can be thermodynamically discriminated at the β-adrenergic receptor. Subsequently, several radioligand binding studies at the cholecystokinin CCK_2 receptor (Harper et al., 2007b), β-adrenergic receptor (Weiland et al., 1979; Contreras et al., 1986a,b), serotonin 5-HT_{1A}-receptor (Dalpiaz et al., 1996), histamine H_3 receptor (Harper et al., 2007a), dopamine D_2 receptor (Kilpatrick et al., 1986; Duarte et al., 1988) and adenosine A_1 and A_{2A} receptors (Borea et al., 1996) were performed at different temperatures to determine thermodynamic parameters such as binding enthalpy ($\Delta H°$) and binding entropy ($\Delta S°$) of the ligand to the receptor. These studies showed that a thermodynamic discrimination between agonism and antagonism is only possible at some of the receptors (e.g., β-adrenergic receptor, 5-HT_3, A_1, and A_{2A} receptors). However, for some receptors, such as the D_2 (Kilpatrick et al., 1986; Duarte et al., 1988) and 5-HT_{1A} (Dalpiaz et al., 1996) receptors, no thermodynamic discrimination between agonists and antagonists was found.

Previous studies from our laboratory (Seifert et al., 2003; Strasser et al., 2008) revealed substantial species differences in affinity between hH_1R and gpH_1R for some H_1R agonists, such as suprahistaprodifen **19**, phenoprodifen **20**, and dimeric hi-

This work was supported by the Research Training Program (Graduiertenkolleg) [Grant GRK760] "Medicinal Chemistry: Molecular Recognition—Ligand-Receptor Interactions" of the Deutsche Forschungsgemeinschaft.
Article, publication date, and citation information can be found at http://molpharm.aspetjournals.org.
doi:10.1124/mol.109.055384.

ABBREVIATIONS: H_1R, histamine H_1-receptor; gp, guinea pig; h, human; GPCR, G-protein coupled receptor; 5-HT, 5-hydroxytryptamine; 3D-QSAR, three-dimensional quantitative structure activity relationship.

staprodifen **22**, and for the first-generation H_1R antagonist mepyramine **1**. Several mutational studies identified amino acids interacting with antagonists in the H_1R binding pocket (Wieland et al., 1999) and amino acids responsible for species differences between hH_1R and gpH_1R (Bruysters et al., 2005; Strasser et al., 2008b) concerning agonists. Because there has been no thermodynamic study of ligand binding to the H_1R, the aim of this study was to analyze the following questions: 1) Is there a thermodynamic discrimination between agonists and antagonists at hH_1R and gpH_1R? 2) Are there species differences in $\Delta H°$ and $\Delta S°$ between hH_1R and gpH_1R?

To answer those two questions, we coexpressed hH_1R or gpH_1R with the regulator of G-protein signaling RGS4 in Sf9 insect cells and characterized a broad spectrum of H_1R agonists, such as phenylhistamines, histaprodifens, and phenoprodifens, as well as H_1R antagonists, such as flexible and tricylic antagonists in [^{3}H]mepyramine competition binding assays at five different temperatures in a temperature range from 283.15 to 303.15 K. In addition, we did not use the van't Hoff equation to determine the binding enthalpy and entropy, as is usually the case. Instead, we used a more general thermodynamic equation that also takes into account the possibility that binding enthalpy and entropy could be temperature-dependent.

Because we included ligands, such as suprahistaprodifen **19**, phenoprodifen **20**, and chiral phenoprodifens **21R** and **21S**, which are predicted to bind in two different orientations to the H_1R (Strasser et al., 2008a, 2009), we additionally performed a temperature-dependent 3D-QSAR analysis to predict thermodynamic properties for orientations 1 and 2.

Materials and Methods

Materials. [^{3}H]Mepyramine (30.0 Ci/mmol) was from PerkinElmer Life and Analytical Sciences (Waltham, MA). Rotiszint Eco Plus scin-

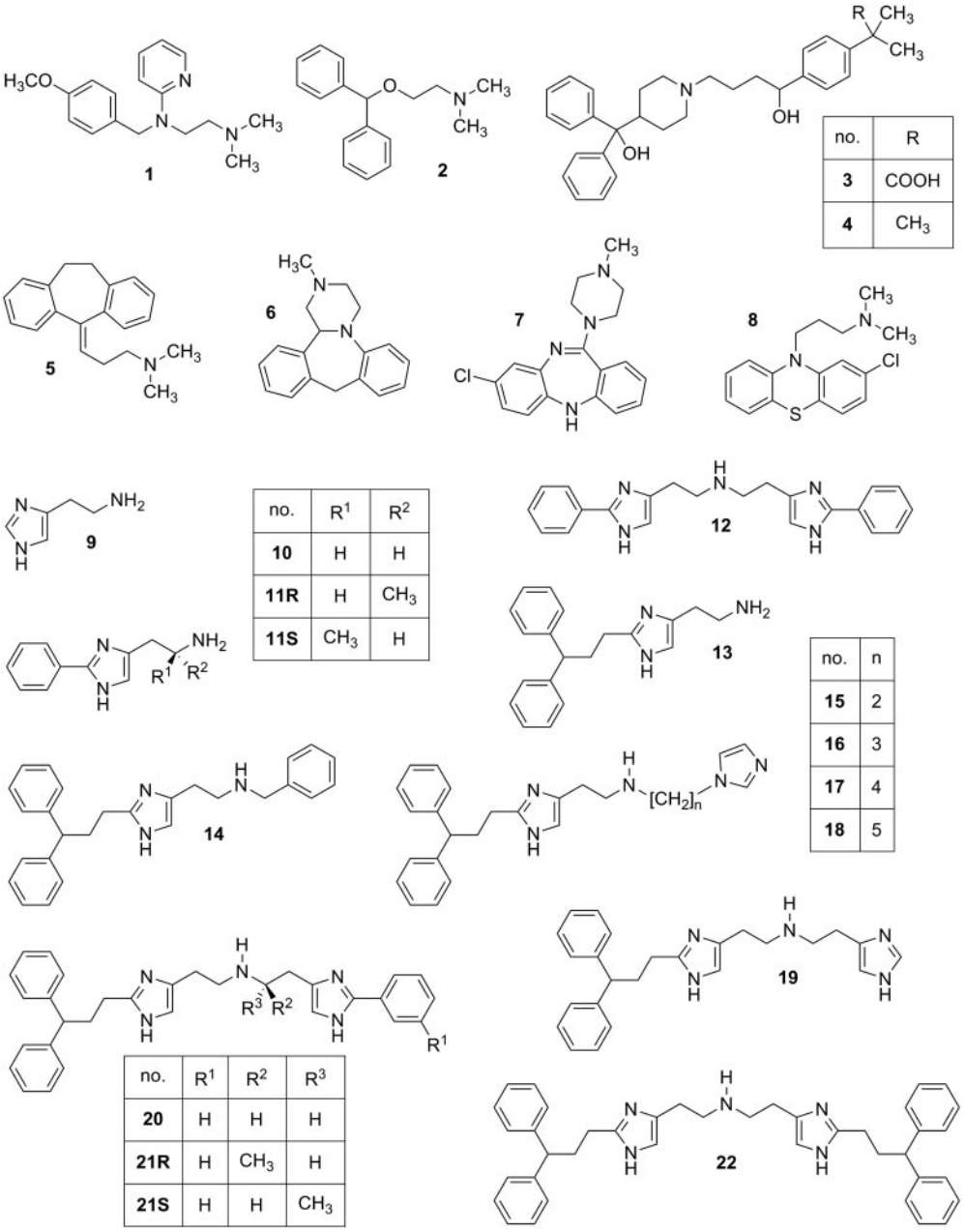

Fig. 1. Chemical structures of H_1R antagonists (**1**-**8**) and H_1R agonists. **1**, mepyramine; **2**, diphenhydramine; **3**, fexofenadine; **4**, terfenadine; **5**, amitriptyline; **6**, mianserin; **7**, clozapine; **8**, chlorpromazine; **9**, histamine; **10**-**12**, phenylhistamines; **13**-**18**, histaprodifens; **19**, suprahistaprodifen; **20** and **21**, phenoprodifens; and **22**, dimeric histaprodifen.

tillation cocktail was from Roth (Karlruhe, Germany). Compounds **1** to **8** were from Sigma (St. Louis, MO). Compound **14** was synthesized as described previously (Menghin, 2004). Sources of all other materials were described previously (Seifert et al., 2003; Strasser et al., 2008a,b, 2009).

Preparation of Compound Stock Solutions. All chemical structures of the analyzed compounds are given in Fig. 1. Compounds **1**, **2**, **9**, **10**, **11R**, and **11S** (10 mM each) were dissolved in double-distilled water. Compounds **3** to **8** (1 mM each) and **12** (5 mM) were dissolved in a solvent containing 50% (v/v) DMSO and 50% (v/v) double-distilled water. Compounds **13** and **15** to **21** (5 mM each) were dissolved in a solvent containing 30% (v/v) DMSO, 30% (v/v) Tris/HCl, pH 7.4 (10 mM), and 40% (v/v) double-distilled water. Compounds **14** and **22** (1 mM) were dissolved in 50% (v/v) DMSO and 50% (v/v) Tris/HCl, pH 7.4 (10 mM). The final DMSO concentration in all assays was adjusted to 3% (v/v) or 5% (v/v) as appropriate for a given compound.

Competition Binding Assays. The [^{3}H]mepyramine competition binding assays were performed as described previously (Strasser et al., 2008a). The assays were carried out two to four times each at temperatures of 283.15, 288.15, 293.15, 298.15, and 303.15 K and, for some compounds, 308.15 K. The temperature was held constant to ±0.1°C, using a water thermostat. To guarantee equilibrium, we carried out preliminary experiments at different incubation times for all ligands at all temperatures. Based on these data, we determined incubation times of 4 h at 283.15 K, 3.5 h at 288.15 K, 1.5 h at 293.15 K and 298.15 K, and 1 h at 303.15 K to ensure equilibrium conditions.

Binding Mode of Dimeric Histaprodifen. Dimeric histaprodifen (**22**) in its bioactive conformation at hH_1R and gpH_1R, resulting from molecular dynamics simulations (Strasser et al., 2008b), was used as template structure for the molecular alignment of all other ligands in the 3D-QSAR study: the quaternary amine moiety, located in the center of dimeric histaprodifen, establishes an electrostatic interaction to Asp$^{3.32}$ and Tyr$^{7.43}$. One imidazole moiety forms stable hydrogen bonds to Ser$^{3.36}$ and Tyr$^{6.51}$, and the second imidazole moiety forms stable hydrogen bonds to Glu190 (E2-loop) and Trp$^{7.40}$. There were no differences in hydrogen bond networking of dimeric histaprodifen **22** with hH_1R and gpH_1R. Both diphenyl propyl moieties of **22** are embedded in hydrophobic pockets.

3D-QSAR. The 3D-QSAR calculations concerning histamine **9**, phenylhistamines **10** to **12**, histaprodifens **13** to **19** and **22,** and phenoprodifens **20**, **21R**, and **21S** were performed with the software package SYBYL (ver. 7.0; Tripos, St. Louis, MO). In the training set we included all ligands with only one possible orientation in the binding pocket (i.e., compounds **9**-**18** and **22**). In the test sets, we included all ligands with two possible orientations (i.e., compounds **19**, **20**, **21R**, and **21S**). The classification of the ligands in a group with one possible orientation and a group with two possible orientations is based on the following considerations: suprahistaprodifen **19** is a substructure of dimeric histaprodifen **22** and should therefore be able to bind in two different orientations. Dimeric phenylhistamine **12** and dimeric histaprodifen **22** bind to the H_1R, and thus phenoprodifens **20**, **21R**, and **21S**, containing a phenylhistamine and histaprodifen partial structure, should be able to bind in two different orientations into the binding-pocket of the H_1R. Besides, both orientations of **20** led to stable ligand-receptor complexes in molecular dynamics simulations (Strasser et al., 2009). This considerations concerning symmetry of the ligands are not valid for ligands **15** to **18**. Accordingly, these ligands are expected to bind in only one orientation. We used dimeric histaprodifen **22** in its bioactive conformation at hH_1R and gpH_1R, resulting of molecular dynamics simulations, as template structure for the molecular alignment of all other ligands (Strasser et al., 2008b). All other ligands were constructed with SYBYL, except for histamine **9**. Because the binding mode of histamine **9** differs from the binding mode of the histamine partial structures in phenylhistamines and histaprodifens, histamine was docked manually in its bioactive conformation as described previously (Jongejan et al., 2005) to hH_1R and gpH_1R using SYBYL. All ligands have one positive charge on the amine moiety. For energetic calculations and minimizations, we used the Tripos-Force-Field and Gasteiger-Hückel partial charges. The alignment was performed with SYBYL using the MultiFit tool. All compounds that can bind in two different orientations in the binding-pocket were aligned in both orientations. This alignment was used for the subsequent comparative molecular field analysis study for each temperature at hH_1R and gpH_1R. The relationship between the ligand structure and the affinities was quantified by the partial least-square (PLS) algorithm (Wold et al., 1993). The cross-validation analysis was performed using the leave-one-out method. In most cases of single 3D-QSAR studies at each temperature for hH_1R and gpH_1R, the cross-validated r^2 resulted in an optimum number of six components for lowest standard error of prediction. Thus, to obtain comparable results for each 3D-QSAR study, we used six components for the subsequent PLS analysis. The predicted pK_i values were used to calculate the thermodynamic parameters $\Delta H°(p,T_o)$, $\Delta S°(p,T_o)$, and ΔC_p° as described in the next paragraph.

Calculation of Thermodynamic Parameters. For the ligand receptor binding equilibrium L + R ⇋ LR (L = ligand, R = receptor, LR = ligand-receptor-complex), the affinity constants are calculated as

$$K_A = \frac{[LR]}{([L][R])} \tag{1}$$

Ligand-receptor binding at constant temperature T and pressure p is accompanied by a decrease of the Gibbs energy of the system, composed of the solvent, the free ligand, and membrane-bound receptor and ligand-receptor-complex, until equilibrium is reached. The resulting equilibrium constant for the association process K_A is related to the change of Gibbs energy of reference state (infinite dilution for each reactant):

$$\Delta G°(p,T) = -RT\ln(K_A), \tag{2}$$

where R is the gas constant.

The binding enthalpy $\Delta H°$ and binding entropy $\Delta S°$ are related to $\Delta G°$ in the following way:

$$\Delta G°(p,T) = \Delta H°(p,T) - T\Delta S°(p,T) \tag{3}$$

The binding enthalpy $\Delta H°(p,T)$ and binding entropy $\Delta S°(p,T)$ are related to enthalpies and entropies of ligand H_L, S_L, of receptor H_R, S_R and of ligand-receptor-complex H_{LR}, S_{LR}, respectively in the following way:

$$\Delta H°(p,T_o) = H_{LR}^\circ - H_L^\circ - H_R^\circ \tag{4}$$

and

$$\Delta S°(p,T_o) = S_{LR}^\circ - S_L^\circ - S_R^\circ \tag{5}$$

In the case of temperature-independent binding enthalpy and binding entropy change, these quantities can be calculated by using the van't Hoff equation:

$$\ln(K_A) = \frac{-\Delta H°(p,T)}{RT} + \frac{\Delta S°(p,T)}{R} \tag{6}$$

In the case of temperature-dependent $\Delta H°$ and $\Delta S°$, we used the following fundamental thermodynamic relations for calculation of these quantities:

$$\left(\frac{\partial \Delta H°(p,T)}{\partial T}\right)_p = \Delta C_p^\circ(p,T) \tag{7}$$

and

$$\left(\frac{\partial \Delta S°(p,T)}{\partial T}\right)_p = \frac{\Delta C_p^\circ(p,T)}{T} \tag{8}$$

where ΔC_p° represents the change in the reference molar heat capacity of the given reaction. Considering this quantity to be temperature-independent as a first approximation, we yield the following relations for $\Delta H°(p,T)$ and $\Delta S°(p,T)$ by integration:

$$\Delta H°(p,T) = \Delta H°(p,T_o) + \Delta C_p^\circ(p,T_o) \cdot (T - T_o) \quad (9)$$

and

$$\Delta S°(p,T) = \Delta S°(p,T_o) + \Delta C_p^\circ(p,T_o) \cdot \ln\left(\frac{T}{T_o}\right) \quad (10)$$

with the reference temperature T_o = 293.15 K.

Using eqs. 3, 9, and 10, the following expression for $\Delta G°(p,T)$ can be derived

$$\Delta G°(p,T) = \Delta H°(p,T_o) + \Delta C_p^\circ(p,T_o) \cdot (T - T_o) - T \cdot \left(\Delta S°(p,T_o) + \Delta C_p^\circ(p,T_o) \cdot \ln\left(\frac{T}{T_o}\right)\right) \quad (11)$$

Using the experimentally determined pK_i values at a pressure p of 101,325 Pa and different temperatures, the quantities $\Delta H°(p,T_o)$, $\Delta S°(p,T_o)$, and $\Delta C_p^\circ(p,T_o)$ can be calculated based on the last equation by a linear least-squares algorithm.

Miscellaneous. The generation of baculoviruses used was described previously (Seifert et al., 2003; Strasser et al., 2008). Cell culture, membrane preparation and determination of protein concentration were performed as described previously (Kelley et al., 2001; Seifert et al., 2003; Strasser et al., 2008a). For data analysis, the software Prism 4.02 (GraphPad Software, San Diego, CA) was used. pK_i values were calculated according to Cheng and Prusoff (1973). All pK_i values are the means ± S.E.M. of two to four independent experiments. For comparison of two pairs of data, the significance of the deviation of zero p was calculated using the t test.

Results

Ligand- and Receptor-Specific Differences in Temperature Dependence of pK_i Values. The pK_i values determined for hH_1R and gpH_1R at five temperatures in the range between 283.15 and 303.15 K (308.15 K for **1**, **4**, **5**, and **7**) are summarized in Table 1 and plotted in Fig. 2. pK_i values exhibited ligand- and receptor-specific differences in temperature dependence. The H_1R antagonists **1** – **8** showed high affinity to hH_1R and gpH_1R within the analyzed temperature range from 283.15 K to 303.15 (308.15 for **1**, **4**, **5** and **7**). Mepyramine **1**, diphenhydramine **2,** and chlorpromazine **8** showed no significant temperature-dependence in affinity. However, some ligands showed a substantial temperature-dependence in affinity, such as fexofenadine **3**, terfenadine **4,** and clozapine **7**. For clozapine **7** (Fig. 3), the increase in affinity from 283.15 to 308.15 K was approximately 1 unit in pK_i. Most of the ligands showed no species-dependent differences in temperature-dependence of affinities. Nonetheless, for the rigid tricyclic ligands amitriptyline **5**, mianserin **6**, and clozapine **7**, the temperature dependence of pK_i values was larger at gpH_1R than at hH_1R. For these ligands, a temperature-dependent selectivity switch between hH_1R and gpH_1R was observed. At 283.15 K, ligands **5** to **7** exhibited higher affinity to hH_1R than to gpH_1R, but at 303.15 K (for **6** and **7**) and 308.15 K (for **5**), the ligands exhibited higher affinity to gpH_1R than to hH_1R. This was most pronounced for amitriptyline **5** (Fig. 4). At temperatures below 295 K, amitriptyline **5** showed higher affinity at hH_1R than at gpH_1R; at a temperature of approximately 295 K, there were no differences in affinity between hH_1R and gpH_1R. At temperatures above 295 K, however, amitriptyline **5** showed higher affinity at gpH_1R than at hH_1R.

The affinities of histamine, phenylhistamines, histaprodifens, and chiraprodifens were in a pK_i range from approximately 4 to 7. In general, these ligands **10** to **22** showed no temperature-dependence in affinity or increasing affinity with increasing temperature, except for histamine **9**. The affinity of histamine **9** decreased slightly with increasing temperature (Fig. 2). For the ligands **9** to **11**, **13** to **18**, and **21R**, no species differences between hH_1R and gpH_1R at the different temperatures were found. Nonetheless, there were species differences at several temperatures for compounds **12**, **19**, **20**, **21S**, and **22**. These species differences were not significantly temperature dependent.

Ligand- and Receptor-Specific Differences in Thermodynamic Parameters of Ligand Binding. All thermodynamic parameters were calculated with Prism using eq. 11 and are given in Table 2. Enthalpy ranged from approximately −35 to 80 kJ/mol at hH_1R and from approximately −25 to 100 kJ/mol at gpH_1R. Entropy ranged from approximately −20 to 410 J/K mol^{-1} at hH_1R and from approximately 20 to 500 J/K mol^{-1} at gpH_1R. The data show that the enthalpy for formation of the ligand-receptor complex at gpH_1R is nearly equal or up to 40 kJ/mol higher than at hH_1R. In addition, the entropy for formation of the ligand-receptor complex at gpH_1R was nearly equal or up to 135 J/K mol^{-1} higher than at hH_1R. This implies that $-T\Delta S°$ at gpH_1R is nearly equal or up to −40 kJ/mol smaller than at hH_1R at a temperature of 293.15 K. A correlation between $\Delta H°$ and $-T\Delta S°$ (Fig. 5) shows that, in general, the formation of the ligand-receptor complex is entropy-driven at hH_1R and gpH_1R. It is noteworthy that, at hH_1R, the formation of some ligand-receptor complexes was not only entropy-driven but also slightly enthalpy-driven. A completely different behavior with regard to the mentioned trend was observed for histamine **9**. At hH_1R and gpH_1R, the formation of the histamine-receptor complex is enthalpy-driven but not or only slightly entropy-driven at a temperature of 293.15 K. Thus, only for the endogenous ligand histamine **9** is the formation of the ligand-receptor complex significantly enthalpy-driven at 293.15 K. As Fig. 5 shows, for hH_1R and gpH_1R, it is not possible to discriminate between agonism and antagonism based on thermodynamical data. The antagonists fexofenadine **3**, terfenadine **4**, mianserine **6**, and clozapine **7** showed very high $\Delta H°(p,T_o)$ and $\Delta S°(p,T_o)$ at hH_1R and gpH_1R, outside the region in which most of the ligands located. This may be explained with specific solvent effects for **3** and **4** or the ligand rigidity for **6** and **7**.

As shown in Table 2, ΔC_p°-values ranged between −5 and 5 kJ/mol K^{-1} and are different from zero for some ligand-receptor systems. Consequently, the enthalpy and entropy of formation of the ligand-receptor complex is temperature-dependent for these systems (e.g., for the formation of the dimeric histaprodifen **22**-gpH_1R receptor complex). If ΔC_p° is zero, $\Delta H°$ and $\Delta S°$ are independent of temperature, resulting in a linear temperature dependence for $\Delta G°$. However, as can be seen in Fig. 6, $\Delta G°$ was not linearly dependent on temperature for dimeric histaprodifen **22** at gpH_1R, indicating a ΔC_p° different from zero. However, it should be noted that for many compounds, the errors in ΔC_p° values are in the same range as the ΔC_p° values themselves. This is a consequence of

TABLE 1

pK_i values for H_1-receptor antagonists and agonists at hH_1R and gpH_1R coexpressed with RGS4 in Sf9 cell membranes in the competition binding assays at different temperatures

[^{3}H]Mepyramine competition binding assays in Sf9 membranes expressing hH_1R or gpH_1R in combination with RGS4 were performed at different temperatures in presence of 5 nM [^{3}H]mepyramine as described under *Materials and Methods*. Data were analyzed by non-linear regression and were best fit to one-site (monophasic) competition curves. pK_i values were calculated according to Cheng and Prusoff (1973). Data shown are the means ± S.E.M. of at least two to four experiments with independent membrane preparations in duplicates each.

Compound and H_1R Species	283 K	288 K	293 K	298 K	303 K	308 K
1						
Human	8.33 ± 0.03	8.35 ± 0.03	8.35 ± 0.03	8.33 ± 0.03	8.31 ± 0.03	8.32 ± 0.02
Guinea pig	8.57 ± 0.02	8.59 ± 0.02	8.58 ± 0.03	8.58 ± 0.03	8.60 ± 0.02	8.58 ± 0.03
2						
Human	7.67 ± 0.05	7.67 ± 0.06	7.83 ± 0.03	7.78 ± 0.03	7.95 ± 0.03	
Guinea pig	7.52 ± 0.03	7.57 ± 0.07	7.53 ± 0.04	7.66 ± 0.01	7.78 ± 0.01	
3						
Human	6.77 ± 0.07	6.93 ± 0.08	7.23 ± 0.11	7.45 ± 0.07	7.73 ± 0.08	
Guinea pig	6.39 ± 0.10	6.51 ± 0.06	6.83 ± 0.04	7.08 ± 0.07	7.42 ± 0.04	
4						
Human	7.66 ± 0.09	7.76 ± 0.08	8.05 ± 0.01	8.22 ± 0.01	8.41 ± 0.06	8.70 ± 0.02
Guinea pig	7.39 ± 0.09	7.45 ± 0.09	7.52 ± 0.07	7.96 ± 0.03	8.21 ± 0.11	8.37 ± 0.08
5						
Human	8.78 ± 0.04	8.94 ± 0.01	8.89 ± 0.04	9.04 ± 0.06	8.99 ± 0.04	8.96 ± 0.07
Guinea pig	8.60 ± 0.02	8.82 ± 0.01	8.86 ± 0.06	9.01 ± 0.04	9.22 ± 0.01	9.22 ± 0.06
6						
Human	8.62 ± 0.02	8.67 ± 0.02	8.81 ± 0.05	8.92 ± 0.02	8.99 ± 0.04	
Guinea pig	8.52 ± 0.01	8.57 ± 0.05	8.81 ± 0.06	9.08 ± 0.07	9.32 ± 0.06	
7						
Human	8.01 ± 0.03	8.29 ± 0.09	8.50 ± 0.06	8.87 ± 0.04	8.80 ± 0.08	9.05 ± 0.06
Guinea pig	7.71 ± 0.02	8.07 ± 0.01	8.25 ± 0.06	8.82 ± 0.08	8.96 ± 0.04	9.09 ± 0.13
8						
Human	7.91 ± 0.03	7.89 ± 0.05	7.83 ± 0.03	7.81 ± 0.02	7.91 ± 0.04	
Guinea pig	7.93 ± 0.07	7.97 ± 0.01	8.09 ± 0.06	8.16 ± 0.06	8.22 ± 0.01	
9						
Human	5.75 ± 0.10	5.77 ± 0.06	5.66 ± 0.04	5.48 ± 0.02	5.35 ± 0.05	
Guinea pig	5.75 ± 0.05	5.58 ± 0.04	5.50 ± 0.03	5.49 ± 0.01	5.42 ± 0.04	
10						
Human	5.36 ± 0.03	5.32 ± 0.01	5.38 ± 0.08	5.48 ± 0.03	5.28 ± 0.05	
Guinea pig	5.58 ± 0.10	5.58 ± 0.01	5.63 ± 0.02	5.72 ± 0.02	5.69 ± 0.02	
11R						
Human	4.29 ± 0.01	4.38 ± 0.03	4.50 ± 0.02	4.46 ± 0.06	4.48 ± 0.03	
Guinea pig	4.65 ± 0.01	4.70 ± 0.02	4.71 ± 0.03	4.77 ± 0.03	4.87 ± 0.01	
11S						
Human	5.24 ± 0.03	5.20 ± 0.03	5.18 ± 0.03	5.17 ± 0.04	5.16 ± 0.03	
Guinea pig	5.50 ± 0.02	5.47 ± 0.02	5.45 ± 0.02	5.42 ± 0.02	5.44 ± 0.01	
12						
Human	5.39 ± 0.04	5.42 ± 0.03	5.45 ± 0.03	5.43 ± 0.02	5.46 ± 0.08	
Guinea pig	5.82 ± 0.06	5.87 ± 0.04	5.93 ± 0.03	6.04 ± 0.09	6.06 ± 0.12	
13						
Human	6.50 ± 0.04	6.43 ± 0.04	6.45 ± 0.04	6.43 ± 0.01	6.43 ± 0.03	
Guinea pig	6.27 ± 0.04	6.24 ± 0.05	6.37 ± 0.02	6.25 ± 0.04	6.42 ± 0.03	
14						
Human	5.08 ± 0.01	5.15 ± 0.03	5.24 ± 0.02	5.33 ± 0.03	5.39 ± 0.04	
Guinea pig	5.00 ± 0.07	5.09 ± 0.03	5.12 ± 0.04	5.23 ± 0.03	5.29 ± 0.01	
15						
Human	5.79 ± 0.03	5.79 ± 0.04	5.76 ± 0.02	5.76 ± 0.02	5.77 ± 0.04	
Guinea pig	5.78 ± 0.04	5.81 ± 0.03	5.86 ± 0.04	5.89 ± 0.07	5.91 ± 0.11	
16						
Human	5.54 ± 0.02	5.54 ± 0.01	5.56 ± 0.03	5.57 ± 0.02	5.58 ± 0.03	
Guinea pig	5.73 ± 0.01	5.76 ± 0.02	5.79 ± 0.04	5.84 ± 0.06	5.89 ± 0.09	
17						
Human	5.55 ± 0.06	5.44 ± 0.04	5.59 ± 0.04	5.54 ± 0.04	5.53 ± 0.05	
Guinea pig	5.45 ± 0.04	5.52 ± 0.04	5.50 ± 0.05	5.58 ± 0.05	5.59 ± 0.06	
18						
Human	5.39 ± 0.05	5.38 ± 0.02	5.41 ± 0.03	5.44 ± 0.04	5.46 ± 0.01	
Guinea pig	5.69 ± 0.10	5.65 ± 0.05	5.72 ± 0.04	5.73 ± 0.03	5.81 ± 0.06	
19						
Human	6.38 ± 0.05	6.39 ± 0.08	6.35 ± 0.02	6.32 ± 0.11	6.33 ± 0.02	
Guinea pig	7.18 ± 0.04	7.17 ± 0.01	7.14 ± 0.02	7.27 ± 0.05	7.35 ± 0.01	
20						
Human	6.45 ± 0.07	6.59 ± 0.11	6.58 ± 0.02	6.55 ± 0.01	6.55 ± 0.07	
Guinea pig	7.00 ± 0.12	7.23 ± 0.02	7.32 ± 0.01	7.42 ± 0.02	7.35 ± 0.02	
21R						
Human	5.90 ± 0.06	6.01 ± 0.06	6.05 ± 0.02	6.02 ± 0.01	6.07 ± 0.02	
Guinea pig	6.67 ± 0.01	6.68 ± 0.01	6.76 ± 0.02	6.88 ± 0.01	7.10 ± 0.02	
21S						
Human	6.05 ± 0.04	6.15 ± 0.05	6.29 ± 0.03	6.24 ± 0.01	6.28 ± 0.05	
Guinea pig	6.27 ± 0.04	6.18 ± 0.05	6.35 ± 0.04	6.52 ± 0.06	6.72 ± 0.11	
22						
Human	6.42 ± 0.01	6.46 ± 0.02	6.65 ± 0.01	6.64 ± 0.01	6.67 ± 0.01	
Guinea pig	6.94 ± 0.08	7.22 ± 0.01	7.33 ± 0.03	7.42 ± 0.01	7.38 ± 0.06	

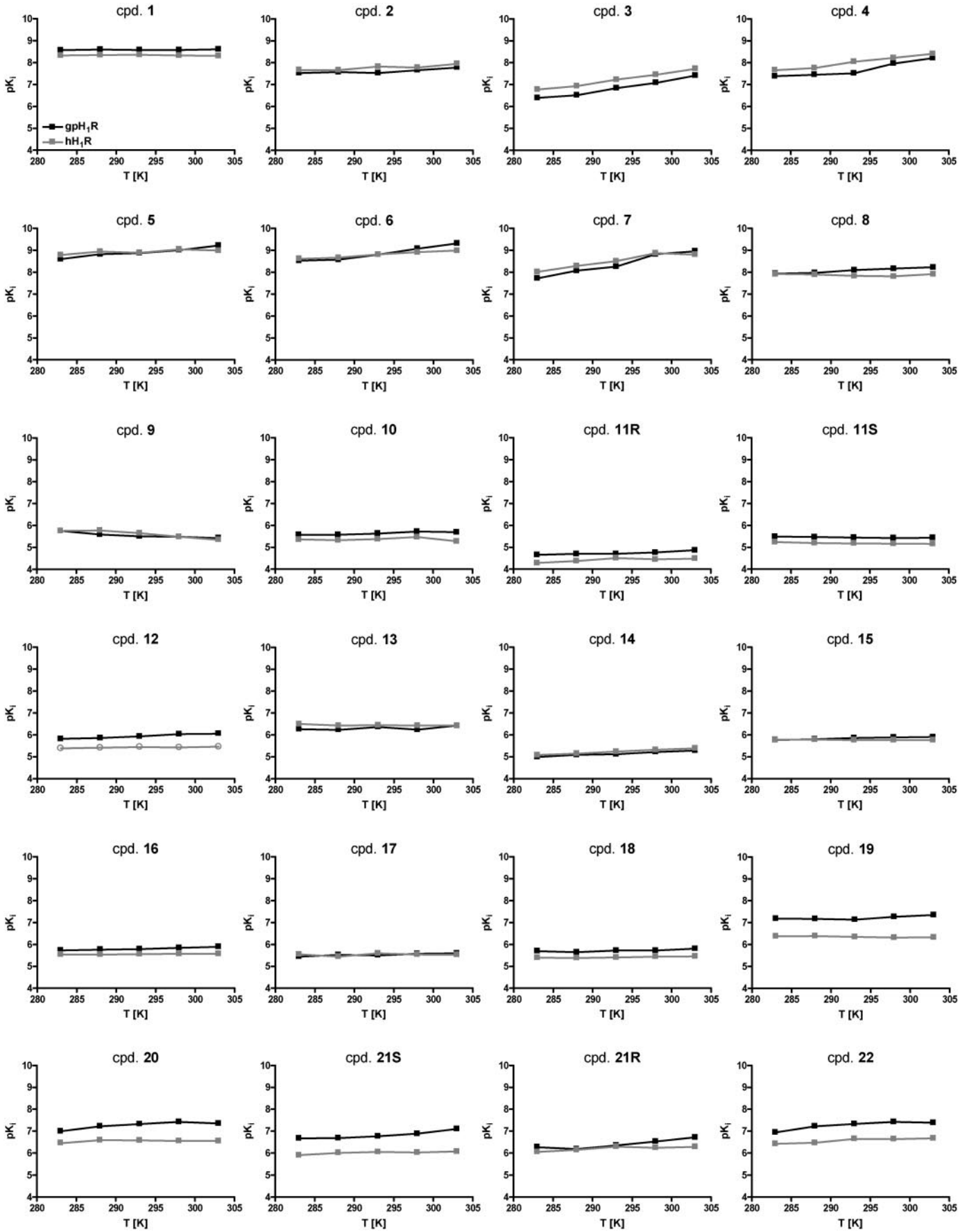

Fig. 2. pK_i values as function of temperature for ligands **1** to **22** at hH_1R and gpH_1R. [^{3}H]Mepyramine competition binding assays in Sf9 membranes expressing hH_1R or gpH_1R in combination with RGS4 were performed at different temperatures in presence of 5 nM [^{3}H]mepyramine as described under *Materials and Methods*. Data were analyzed by nonlinear regression and were best fit to one-site (monophasic) competition curves. pK_i values were calculated according to Cheng and Prusoff (1973). Data shown are the means ± S.E.M. of at least two to four experiments with independent membrane preparations in duplicates each.

a nonattainable precision in measurement of pK_i values. Nonetheless, we used eq. 11 for data analysis because the van't Hoff equation is only a special case of eq. 11. Given this, the data summarized in Table 2 show the trend that ΔC°_p could be higher at gpH_1R, than at hH_1R. Hence, it may be concluded that either enthalpy or entropy of the free gpH_1R or gpH_1R-ligand complex are more temperature-dependent

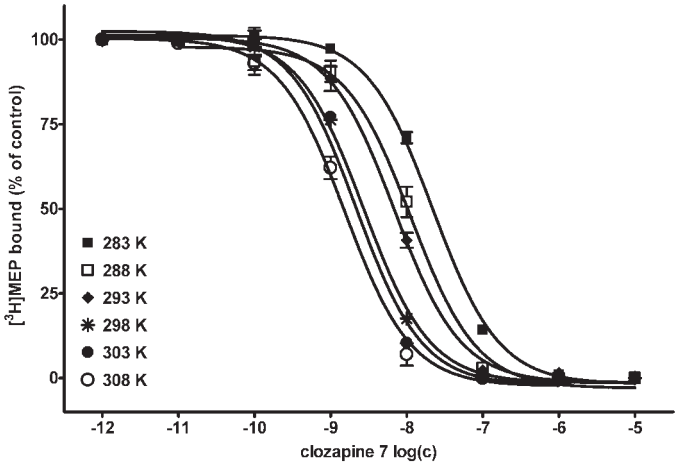

Fig. 3. Competition binding isotherms for clozapine **7** at various temperatures at hH_1R. The experiments were performed using Sf9 cell membranes expressing hH_1R and RGS4 in presence of 5 nM [^{3}H]mepyramine ([^{3}H]MEP) as described under *Materials and Methods*. Data were analyzed by nonlinear regression and were best fit to one-site (monophasic) competition curves.

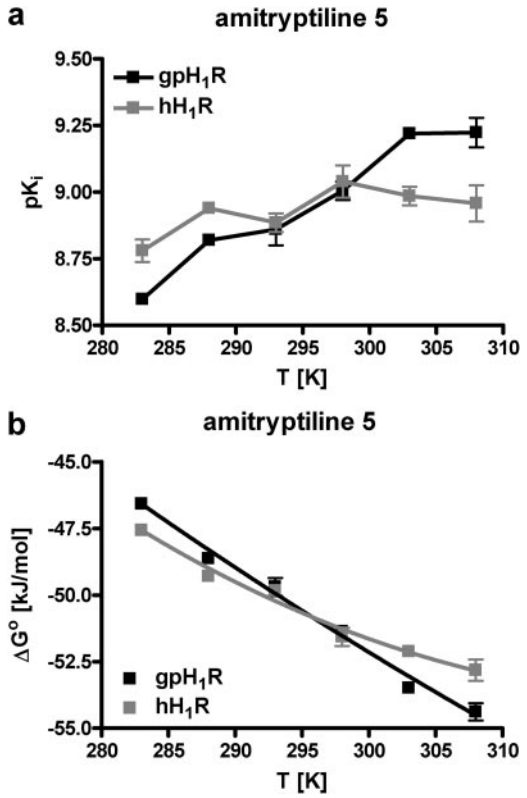

Fig. 4. Temperature-dependence of pK_i and $\Delta G^\circ(p,T)$ for amitriptyline **5** at hH_1R and gpH_1R. a, temperature-dependence of pK_i values for amitriptyline **5** at hH_1R and gpH_1R, based on the data given in Table 2. b, temperature-dependence of $\Delta G^\circ(p,T)$ values for amitriptyline **5** at hH_1R and gpH_1R; the data were calculated using eq. 2 as described under *Materials and Methods*.

than the corresponding parameters at hH_1R. For the D_2 receptor, temperature dependence of binding enthalpy and entropy (Kilpatrick et al., 1986; Duarte et al., 1988) was described for some cases. At the D_2 receptor, ΔC°_p values range between −3 and 3 kJ/mol K^{-1}. A similar phenomenon was also described for the A_1 receptor (Borea et al., 1992; Casado et al., 1993) with values ΔC°_p of approximately −10 and 10 kJ/mol at 293.15 K. Thus, it can be concluded that the heat capacity ΔC°_p should be included into the thermodynamic analysis of ligand-receptor binding in general.

We also calculated ΔH° and $-T\Delta S^\circ$ at 283.15, 288.15, 298.15, and 303.15 K. In the temperature range from 283.15 to 303.15 K, for some ligands, the formation of the ligand-receptor complex switched from enthalpy-driven to entropy-driven and vice versa. For histamine **9**, this switch was species-dependent (Fig. 7).

3D-QSAR. On the one hand, The 3D-QSAR calculations were performed to predict the pK_i values of different orientations. On the other hand, the thermodynamic properties of the ligands should be predicted, especially the contribution of orientations 1 and 2 onto the thermodynamic properties. The alignment of the ligands docked in gpH_1R is shown in Fig. 8. For each 3D-QSAR analysis, the standard error of estimate was smaller than 0.05 in pK_i; r^2 was larger than 0.997 in all 3D-QSAR calculations. The predicted pK_i values for compounds **19** to **21** for orientations 1 and 2 are given in Table 3 at each temperature. Considering the pK_i values for orientations 1 and 2, the effective pK_i values are calculated without any implications about the contribution of orientation 1 or 2. The comparison of predicted, effective pK_i values with the experimental data shows deviations smaller than approximately 0.6 in pK_i.

The predicted thermodynamic parameters for compounds **19**, **20**, **21R**, and **21S** for each orientation are given in Table 4. The prediction of the effective values, including orientations 1 and 2, based on the predicted pK_i values corresponds well to the experimental data for $\Delta H^\circ(p,T_o)$, $\Delta S^\circ(p,T_o)$, and $\Delta G^\circ(p,T_o)$. The prediction of ΔC°_p is not as good as for the other thermodynamic data but is in range of the experimental errors.

Species Differences in Enthalpy and Entropy of the Ligand-Receptor Binding Process. At the reference temperature of 293.15 K, we observed, in general, the trend that $\Delta H^\circ(p,T_o)$ at gpH_1R is equal or higher than at hH_1R. In contrast, $-T\Delta S^\circ(p,T_o)$ at gpH_1R is equal or smaller than at gpH_1R. Consequently, we conclude that the loss in enthalpy at gpH_1R compared with hH_1R is compensated for by an increase in entropy. These species differences are ligand-dependent and are illustrated in Fig. 9. The data shown in Fig. 9 correspond to the equations

$$\Delta\Delta H^\circ(p,T_o)_{gp-h} = \Delta H^\circ(p,T_o)_{gp} - \Delta H^\circ(p,T_o)_h = H^\circ_{(gp-L)} - H^\circ_{(h-L)} - H^\circ_{gp} + H^\circ_h \quad (12)$$

and

$$\Delta\Delta S^\circ(p,T_o)_{gp-h} = \Delta S^\circ(p,T_o)_{gp} - \Delta S^\circ(p,T_o)_h = S^\circ_{(gp-L)} - S^\circ_{(h-L)} - S^\circ_{gp} + S^\circ_h \quad (13)$$

Thus, these data include the differences in enthalpies or entropies of ligand-receptor complexes and the free receptors

TABLE 2

Calculated thermodynamic properties for H_1 receptor antagonists and agonists at hH_1R and gpH_1R

All thermodynamic quantities were calculated, as described under *Materials and Methods*, at a reference temperature of T_o = 293.15 K.

Compound and H_1R Species	$\Delta H°(p,T_o)$	$\Delta S°(p,T_o)$	$-T\Delta S°(p,T_o)$	$\Delta C_p^{\circ}(p,T_o)$	$\Delta G^{o,calc}(p,T_o)$	$\Delta G^{o,exp}(p,T_o)$
	kJ/mol	*J/K mol*$^{-1}$	*kJ/mol*	*J/mol K*$^{-1}$	*kJ/mol*	*kJ/mol*
1						
Human	−1.0 ± 2.1	156.2 ± 7.1	−45.8 ± 2.1	−300.7 ± 492.4	−46.8 ± 3.0	−46.8 ± 0.1
Guinea pig	1.0 ± 1.9	167.7 ± 6.6	−49.2 ± 1.9	−200.5 ± 454.5	−48.2 ± 2.7	−48.1 ± 0.1
2						
Human	22.6 ± 5.0	225.7 ± 17.1	−66.2 ± 5.0	1536 ± 1708	−43.6 ± 7.1	−43.9 ± 0.1
Guinea pig	20.9 ± 4.0	216.0 ± 13.5	−63.3 ± 4.0	3023 ± 1348	−40.4 ± 5.6	−42.2 ± 0.2
3						
Human	80.2 ± 7.4	411.6 ± 25.3	−120.7 ± 7.4	2116 ± 2597	−40.5 ± 10.4	−40.5 ± 0.6
Guinea pig	87.1 ± 8.4	427.4 ± 28.5	−125.3 ± 8.4	4281 ± 2863	−38.2 ± 11.9	−38.3 ± 0.2
4						
Human	64.7 ± 5.9	373.9 ± 20.3	−109.6 ± 5.9	1917 ± 1817	−44.9 ± 8.4	−45.1 ± 0.1
Guinea pig	65.3 ± 7.9	369.3 ± 27.1	−108.2 ± 7.9	3500 ± 2174	−42.9 ± 11.2	−42.2 ± 0.4
5						
Human	16.3 ± 4.9	227.1 ± 17.0	−66.6 ± 5.0	−2142 ± 1247	−50.3 ± 7.0	−49.8 ± 0.2
Guinea pig	44.6 ± 3.8	322.7 ± 13.0	−94.6 ± 3.8	−734.1 ± 981.4	−50.0 ± 5.4	−49.7 ± 0.3
6						
Human	32.6 ± 4.0	279.6 ± 13.4	−82.0 ± 3.9	116.7 ± 1251	−49.4 ± 5.6	−49.4 ± 0.3
Guinea pig	72.2 ± 6.7	415.1 ± 23.0	−121.7 ± 6.7	3943 ± 2221	−49.5 ± 9.5	−49.4 ± 0.3
7						
Human	72.0 ± 4.7	409.0 ± 16.3	−119.9 ± 4.8	−2290 ± 1300	−47.9 ± 6.7	−47.7 ± 0.3
Guinea pig	98.8 ± 5.9	497.8 ± 20.3	−145.9 ± 6.0	−1756 ± 1571	−47.1 ± 8.4	−46.3 ± 0.3
8						
Human	−1.5 ± 3.5	144.7 ± 12.0	−42.4 ± 3.5	2772 ± 1186	−43.9 ± 4.9	−43.9 ± 0.1
Guinea pig	25.9 ± 6.4	242.9 ± 21.9	−71.2 ± 6.4	102.2 ± 1936	−45.3 ± 9.1	−45.4 ± 0.3
9						
Human	−37.6 ± 7.0	−19.9 ± 23.8	5.8 ± 7.0	−3847 ± 2366	−31.8 ± 9.9	−31.7 ± 0.2
Guinea pig	−24.1 ± 4.2	23.3 ± 14.3	−6.8 ± 4.2	2474 ± 1543	−30.9 ± 5.9	−30.9 ± 0.1
10						
Human	−2.1 ± 6.9	96.5 ± 23.2	−28.3 ± 6.8	−2984 ± 2271	−30.4 ± 9.7	−30.2 ± 0.4
Guinea pig	12.1 ± 4.4	149.3 ± 15.0	−43.8 ± 4.4	−125.9 ± 1483	−31.7 ± 6.2	−31.6 ± 0.1
11R						
Human	14.5 ± 3.5	134.9 ± 12.1	−39.5 ± 3.5	−2707 ± 1192	−25.0 ± 4.9	−25.2 ± 0.1
Guinea pig	17.3 ± 2.1	149.3 ± 7.2	−43.8 ± 2.1	1627 ± 709.6	−26.5 ± 3.0	−26.4 ± 0.1
11S						
Human	−6.2 ± 2.5	77.9 ± 8.5	−22.8 ± 2.5	565.2 ± 842.6	−29.0 ± 3.5	−29.0 ± 0.1
Guinea pig	−4.8 ± 1.6	87.7 ± 5.4	−25.7 ± 1.6	767.7 ± 534.1	−30.5 ± 2.3	−30.6 ± 0.1
12						
Human	5.3 ± 4.0	122.0 ± 13.8	−35.8 ± 4.0	−473.6 ± 1361	−30.5 ± 5.7	−30.6 ± 0.2
Guinea pig	21.4 ± 6.8	186.8 ± 23.1	−54.8 ± 6.8	133.0 ± 2285	−33.4 ± 9.6	−33.3 ± 0.2
13						
Human	−3.9 ± 3.9	109.9 ± 13.5	−32.2 ± 4.0	1062 ± 1326	−36.1 ± 5.6	−36.2 ± 0.2
Guinea pig	11.1 ± 5.4	158.4 ± 18.3	−46.4 ± 5.4	1568 ± 1834	−35.3 ± 7.6	−35.7 ± 0.1
14						
Human	25.6 ± 2.2	187.6 ± 7.5	−55.0 ± 2.2	64.9 ± 703.7	−29.4 ± 3.5	−29.4 ± 0.1
Guinea pig	23.6 ± 3.5	178.8 ± 12.1	−52.4 ± 3.5	209.9 ± 1194	−28.8 ± 4.9	−28.7 ± 0.2
15						
Human	−2.3 ± 2.9	102.5 ± 9.9	−30.0 ± 2.9	408.9 ± 982.2	−32.3 ± 4.1	−32.3 ± 0.2
Guinea pig	11.1 ± 5.5	149.8 ± 18.7	−43.9 ± 5.5	−303.1 ± 1843	−32.8 ± 7.8	−32.8 ± 0.2
16						
Human	3.6 ± 1.8	118.7 ± 6.1	−34.8 ± 1.8	22.1 ± 601.8	−31.2 ± 2.5	−31.2 ± 0.1
Guinea pig	13.4 ± 4.7	156.6 ± 16.0	−45.9 ± 4.7	746.9 ± 1580	−32.5 ± 6.6	−32.5 ± 0.2
17						
Human	1.9 ± 5.6	112.5 ± 19.1	−33.0 ± 5.6	−108.7 ± 1887	−31.1 ± 7.9	−31.3 ± 0.2
Guinea pig	11.1 ± 4.3	143.7 ± 14.6	−42.1 ± 4.3	−202.8 ± 1439	−31.0 ± 6.1	−30.9 ± 0.3
18						
Human	6.4 ± 3.0	125.4 ± 10.1	−36.8 ± 3.0	505.0 ± 993.6	−30.4 ± 4.2	−30.3 ± 0.2
Guinea pig	10.6 ± 5.3	145.2 ± 18.1	−42.6 ± 5.3	1801 ± 1786	−32.2 ± 7.5	−32.1 ± 0.2
19						
Human	−5.0 ± 5.7	104.5 ± 19.4	−30.6 ± 5.7	−1.4 ± 1943	−35.6 ± 8.1	−35.6 ± 0.1
Guinea pig	16.1 ± 3.8	192.3 ± 13.0	−56.4 ± 3.8	3350 ± 1215	−40.3 ± 5.4	−40.1 ± 0.1
20						
Human	5.6 ± 6.3	145.4 ± 21.5	−42.6 ± 6.3	−2912 ± 2282	−37.0 ± 8.9	−36.9 ± 0.1
Guinea pig	27.5 ± 4.8	234.5 ± 16.3	−68.7 ± 4.8	−5578 ± 1612	−41.2 ± 6.8	−41.1 ± 0.1
21R						
Human	10.8 ± 4.5	152.3 ± 15.4	−44.6 ± 4.5	−1743 ± 1537	−33.8 ± 6.4	−33.9 ± 0.1
Guinea pig	36.2 ± 1.3	252.9 ± 4.4	−74.1 ± 1.3	4606 ± 442.5	−37.9 ± 1.8	−37.9 ± 0.1
21S						
Human	17.3 ± 4.2	178.5 ± 14.3	−52.3 ± 4.2	−2734 ± 1411	−35.0 ± 5.9	−35.3 ± 0.2
Guinea pig	41.8 ± 7.0	263.9 ± 23.9	−77.4 ± 7.0	5581 ± 2489	−35.6 ± 9.9	−35.6 ± 0.2
22						
Human	22.6 ± 3.9	203.2 ± 13.4	−59.6 ± 3.9	−2196 ± 1295	−37.0 ± 5.5	−37.3 ± 0.1
Guinea pig	33.6 ± 4.6	255.3 ± 15.7	−74.8 ± 4.6	−5989 ± 1545	−41.2 ± 6.5	−41.1 ± 0.2

for hH_1R and gpH_1R but not enthalpies or entropies for the free ligand. Therefore, the quantities $\Delta\Delta H°(p,T_o)_{gp-h}$ and $-T_o\Delta\Delta S°(p,T_o)_{gp-h}$ are ligand-independent but, relative to each other, dependent on the ligand-receptor-complex.

For mianserin **6**, the largest species difference is observed (Fig. 9, group I). In the next group (Fig. 9, group II) are the tricyclic compounds amitriptyline **5**, clozapine **7**, and chlorpromazine **8**, as well as the histaprodifens, which can bind in two different orientations into the binding pocket, such as suprahistaprodifen **19**, phenoprodifen **20**, and the chiral phenoprodifens **21R** and **21S**. In group III (Fig. 9), ligands with enthalpic species differences in a range from −9 to −16 kJ/mol, and entropic species differences in a range from −9 to −19 kJ/mol are found. These ligands include histamine **9**, phenylhistamine **10**, dimeric phenylhistamine **11**, histaprodifen **13**, and the histaprodifen derivatives **15** to **17** and **22**. The last group (Fig. 9, group IV), with smaller enthalpic and entropic species differences in a range from −5 to 5 kJ/mol, comprises the flexible antagonists **1** to **4**, the chiral phenylhistamines **11R** and **11S**, and the histaprodifen derivatives **14** and **18**. The location of the effective enthalpic and entropic species differences between hH_1R and gpH_1R for **19**, **20**, **21R**,

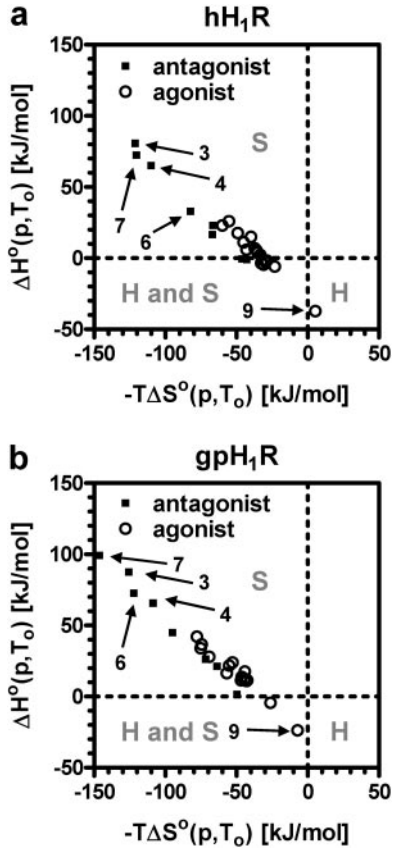

Fig. 5. Scatter plot of $\Delta H°(p,T_o)$ versus $-T\Delta S°(p,T_o)$ for H_1R antagonists and agonists. The data points are given for the temperature 293.15 K and are based on Table 2. Region *H*, enthalpy-driven; Region *S*, entropy-driven; Region *H* and *S*, enthalpy- and entropy-driven.

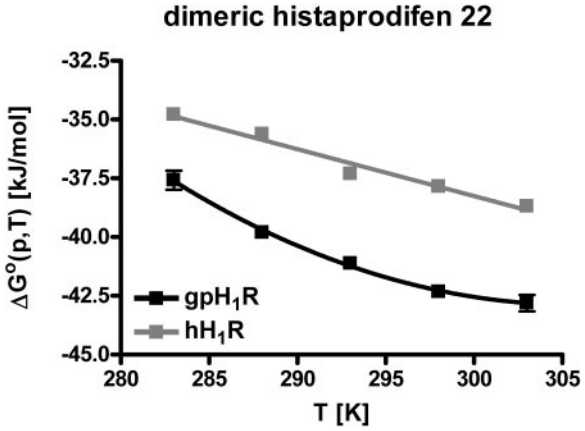

Fig. 6. Temperature-dependence of $\Delta G°(p,T)$ for dimeric histaprodifen 22 at hH_1R and gpH_1R. $\Delta G°$ values at the different temperatures were calculated using eq. 2 as described under *Materials and Methods*, based on the data given in Table 1.

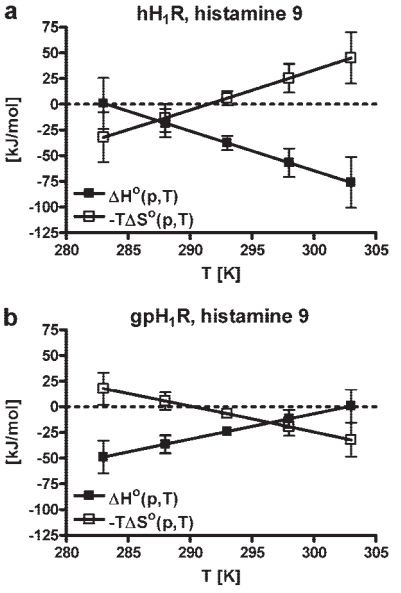

Fig. 7. $\Delta H°(p,T)$ and $-T\Delta S°(p,T)$ as a function of temperature for histamine **9** at hH_1R and gpH_1R. The quantities $\Delta H°(p,T)$ and $-T\Delta S°(p,T)$ were calculated based on the data in Table 2, using the equation $\Delta H°(p,T) = \Delta H°(p,T_o) + \Delta C°_p(p,T_o) \cdot (T - T_o)$ for temperature-dependence of $\Delta H°(p,T)$ and equation $\Delta S°(p,T) = \Delta S°(p,T_o) + \Delta C°_p(p,T_o) \cdot \ln(T/T_o)$ for temperature dependence of $-T\Delta S°(p,T)$.

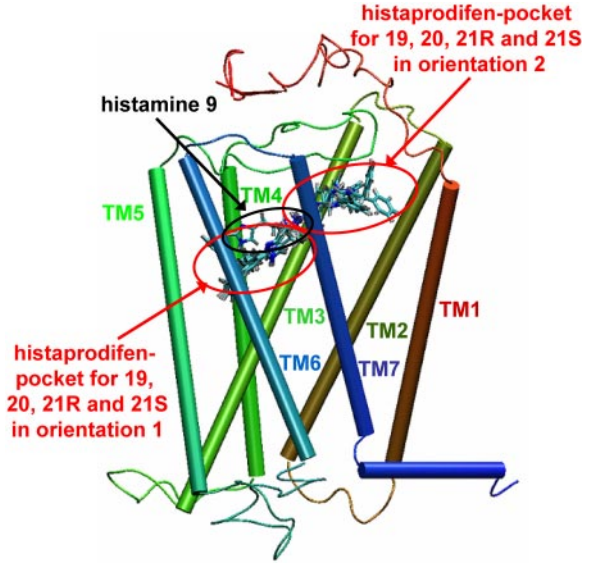

Fig. 8. Alignment of histamine, phenylhistamines, histaprodifens, and phenoprodifens in the active gpH_1R. The alignment was performed as described under *Materials and Methods*.

and **21S** far away from the other phenylhistamines and histaprodifens is a priori unexpected. However the 3D-QSAR prediction with regard to enthalpy and entropy of these ligands for orientations 1 and 2 shows a shift away from the nonflexible antagonists (group II) toward phenylhistamines and histaprodifens (Fig. 9). For **19**, **20**, **21R**, and **21S**, orientation 1 is found in the same group (group III) as histaprodifen and most histaprodifen derivatives. In contrast, for **19** and **20**, orientation 2 is found in the same range (group III) as histamine **9** and phenylhistamine **10**, but for **21R** and **21S** orientation 2 is found in the same range (group IV) as the chiral phenylhistamines **11R** and **11S**, respectively.

The separation of the effective $\Delta\Delta H°(p,T_o)_{gp-h}$ and $-T\Delta\Delta S°(p,T_o)_{gp-h}$ into the predicted data for orientation 1 and 2 (Fig. 9) shows, that for **19**, **20**, **21R**, and **21S** the quantities for orientation 1 are found in group III. In orientation 1, the histaprodifen moieties of **19**, **20**, **21R**, and **21S** are located in the same part of the binding-pocket as histaprodifen **13** itself. In group III, **13** and dimeric histaprodifen **22** are found too. In contrast, for **19**, **20**, **21R**, and **21S**, the quantities for orientation 2 are found in group III only for **19** and **20** but in group IV for **21R** and **21S**. In orientation 2, the histaprodifen moieties of **19**, **20**, **21R**, and **21S** are located not in the histaprodifen binding-pocket itself, but in a pocket possessed by the second histaprodifen moiety of **22**, located near TM2. The histamine moiety of **19** and phenylhistamine moieties of **20**, **21R**, and **21S** in orientation 2 are located in the binding-pocket of histamine **9** and phenylhistamines **10**, **11R**, and **11S** itself. Compounds **9** and **10** are located in group III, as well as orientation 2 of compounds **19** and **20**. In addition, the chiral phenylhistamines **11R** and **11S** belong to group IV, as well as orientation 2 of compounds **21R** and **21S**. Furthermore, the data suggest that there is no change in species difference of $\Delta\Delta H°(p,T_o)_{gp-h}$ and $-T\Delta\Delta S°(p,T_o)_{gp-h}$ in case of introduction of a second phenylhistamine moiety into **10**, resulting in **12**, or in the case of introduction of a second histaprodifen moiety into **13**, resulting in **22**. Based on these data we suggest that the part of the entire binding-pocket of phenylhistamine **10** and histaprodifen **13**, located near to TM5 is responsible for the membership of **19**, **20**, **21R**, and **21S** (Strasser et al., 2009) dependent from orientation to group III or group IV.

Discussion

Thermodynamic Discrimination between Antagonism and Agonism. Previous studies showed that it is possible to discriminate between agonism and antagonism based on binding enthalpy and binding entropy for some GPCRs. Discrimination was found for the β-adrenergic receptor and the A_1 and A_{2A} receptors. The formation of ligand-receptor-complexes is enthalpy-driven for agonists and enthalpy- and

TABLE 3

Predicted pK_i values for suprahistaprodifen **19**, phenoprodifen **20**, and the chiral phenoprodifens **21R** and **21S** based on 3D-QSAR calculations

The calculations were performed as described under *Materials and Methods*. Δ describes the difference pK_i(predicted) − pK_i(experimental). The effective pK_i value (eff), including orientation 1 (or1) and orientation 2 (or2) was calculated using equation $\log_{10}(K_i\ (or1) + K_i\ (or2))$ as described previously (Strasser et al., 2009).

Compound, H_1R Species, Orientation	283 K		288 K		293 K		298 K		303 K	
	Pred.	Δ	Pred.	Δ	Pred.	Δ	Pred.	Δ	Pred.	Δ
19										
Human										
or1	5.95		5.96		6.01		6.01		6.08	
or2	5.45		5.53		5.71		5.71		5.60	
eff	6.07	−0.31	6.10	−0.29	6.19	−0.16	6.19	−0.13	6.20	−0.13
Guinea pig										
or1	6.03		6.07		6.12		6.19		6.26	
or2	6.40		6.48		6.56		6.63		6.70	
eff	6.55	−0.63	6.62	−0.55	6.69	−0.45	6.76	−0.51	6.83	−0.52
20										
Human										
or1	6.43		6.42		6.46		6.43		6.52	
or2	5.42		5.50		5.67		5.68		5.64	
eff	6.47	0.02	6.47	−0.12	6.52	−0.06	6.50	−0.05	6.57	0.02
Guinea pig										
or1	6.56		6.61		6.67		6.76		6.84	
or2	6.41		6.52		6.64		6.74		6.83	
eff	6.79	−0.21	6.87	−0.36	6.95	−0.37	7.05	−0.37	7.14	−0.21
21R										
Human										
or1	5.99		5.98		6.06		6.06		6.09	
or2	4.75		4.91		5.16		5.14		5.14	
eff	6.01	0.11	6.02	0.01	6.11	0.06	6.11	0.09	6.14	0.07
Guinea pig										
or1	6.48		6.54		6.60		6.70		6.76	
or2	5.87		5.99		6.11		6.23		6.25	
eff	6.58	−0.09	6.65	−0.03	6.72	−0.04	6.83	−0.05	6.88	−0.22
21S										
Human										
or1	5.88		5.89		5.98		5.99		6.05	
or2	5.15		5.29		5.52		5.50		5.58	
eff	5.95	−0.10	5.99	−0.16	6.11	−0.18	6.11	−0.13	6.18	−0.10
Guinea pig										
or1	5.98		6.06		6.11		6.22		6.27	
or2	6.20		6.30		6.42		6.55		6.63	
eff	6.40	0.13	6.50	0.32	6.59	0.24	6.72	0.20	6.79	0.07

entropy-driven for antagonists at β-adrenergic receptor (Weiland et al., 1979; Contreras et al., 1986a,b). In contrast, the formation of ligand-receptor-complexes is entropy-driven for agonists and enthalpy- and entropy-driven for antagonists at A_1 receptors (Dalpiaz et al., 1996) and A_{2A} receptors. For the D_2 (Duarte et al., 1988) and 5-HT_{1A} receptor (Dalpiaz et al., 1996), discrimination between agonism and antagonism based on $\Delta H°$ and $\Delta S°$ is not possible. A study on the H_3 receptor (Harper and Black, 2007a) showed that discrimination between agonism and antagonism depends of the experimentally used buffer. $\Delta H°$ is found in a range from approximately −225 to 100 kJ/mol, $\Delta S°$ is in a range from

TABLE 4

Predicted thermodynamic properties for suprahistaprodifen **19**, phenoprodifen **20**, and the chiral phenoprodifens **21R** and **21S** at a temperature of 293.15 K

The thermodynamic parameters are calculated based on the predicted pK_i values (Table 3) as described under *Materials and Methods*. The difference predicted quantity—experimental quantity for the effective quantities is given by Δ.

Compound, H_1R Species, Orientation	$\Delta H°(p,T_o)$		$\Delta S°(p,T_o)$		$-T\Delta S°(p,T_o)$		$\Delta C°_p(p,T_o)$		$\Delta G°(p,T_o)$	
	Pred.	Δ	Pred.	Δ	Pred.	Δ	Pred.	Δ	Pred.	Δ
	kJ/mol		*J/K mol*$^{-1}$		*kJ/mol*		*J/mol K*$^{-1}$		*kJ/mol*	
19										
Human										
or1	10.4 ± 2.0		150.3 ± 6.8		−44.1 ± 2.0		730.5 ± 676.4		−33.7 ± 2.8	
or2	14.0 ± 5.9		156.5 ± 20.2		−45.9 ± 5.9		−5177 ± 2000		−31.9 ± 8.3	
eff	11.1 ± 2.5	16.1	156.0 ± 8.5	51.5	−45.7 ± 2.5	−15.1	−1148 ± 840.1	−1147	−34.6 ± 3.5	1.0
Guinea pig										
or1	19.3 ± 0.3		183.3 ± 1.1		−53.7 ± 0.3		879.9 ± 112.3		−34.4 ± 0.4	
or2	24.6 ± 0.2		209.5 ± 0.6		−61.4 ± 0.2		−113.4 ± 59.5		−36.8 ± 0.3	
eff	23.0 ± 0.1	6.9	206.7 ± 0.1	14.4	−60.6 ± 0.1	−4.2	157.0 ± 0.6	−3193	−37.6 ± 0.1	2.5
20										
Human										
or1	6.3 ± 3.3		144.7 ± 11.1		−42.4 ± 3.3		1457 ± 1100		−36.1 ± 4.7	
or2	19.3 ± 4.9		174.0 ± 16.7		−51.0 ± 4.9		−3745 ± 1653		−31.7 ± 6.9	
eff	7.8 ± 2.9	2.2	151.0 ± 9.8	5.6	−44.3 ± 2.9	−1.7	770.2 ± 967.5	3682	−36.5 ± 4.1	0.4
Guinea pig										
or1	24.1 ± 0.7		209.9 ± 2.3		−61.5 ± 0.7		1108 ± 229.7		−37.4 ± 1.0	
or2	34.7 ± 0.7		245.5 ± 2.5		−72.0 ± 0.7		−244.5 ± 90.46		−37.3 ± 1.0	
eff	29.9 ± 0.5	2.4	235.5 ± 1.7	1.0	−69.0 ± 0.5	−0.3	551.7 ± 126.7	6130	−39.1 ± 0.7	2.0
21R										
Human										
or1	9.2 ± 2.8		147.0 ± 9.6		−43.1 ± 2.8		55.1 ± 945.0		−33.9 ± 4.0	
or2	31.3 ± 6.0		204.7 ± 20.4		−60.0 ± 6.0		−5322 ± 2019		−28.7 ± 8.5	
eff	11.4 ± 2.8	0.6	155.3 ± 9.5	3.0	−45.5 ± 2.8	−0.9	−397.4 ± 940.3	1346	−34.1 ± 4.0	−0.2
Guinea pig										
or1	23.8 ± 1.4		207.9 ± 4.8		−60.9 ± 1.4		532.0 ± 476.7		−37.1 ± 2.0	
or2	32.3 ± 2.6		227.3 ± 8.9		−66.6 ± 2.6		−1666 ± 874.9		−34.3 ± 3.7	
eff	25.7 ± 1.9	−10.5	216.5 ± 6.4	−36.4	−63.5 ± 1.9	10.6	167.3 ± 636.0	−4439	−37.8 ± 2.7	0.1
21S										
Human										
or1	14.5 ± 2.6		163.7 ± 9.0		−48.0 ± 2.6		282.6 ± 886.1		−33.7 ± 3.7	
or2	34.0 ± 6.1		220.7 ± 20.8		−64.7 ± 6.1		−3233 ± 2050		−30.7 ± 8.6	
eff	18.9 ± 3.4	1.6	180.8 ± 11.7	2.3	−53.0 ± 3.4	0.7	−434.5 ± 1159	2300	−34.1 ± 4.8	1.2
Guinea pig										
or1	24.4 ± 2.0		200.4 ± 6.8		−58.7 ± 2.0		162.2 ± 672.1		−34.3 ± 2.8	
or2	36.4 ± 1.7		247.4 ± 5.8		−72.5 ± 1.7		−41.6 ± 576.8		−36.1 ± 2.4	
eff	32.8 ± 1.8	−9.0	238.5 ± 6.1	−25.4	−69.9 ± 1.8	7.5	30.2 ± 602.9	−5551	−37.1 ± 2.6	−1.5

eff, effective pK_i value; or1, orientation 1; or2, orientation 2.

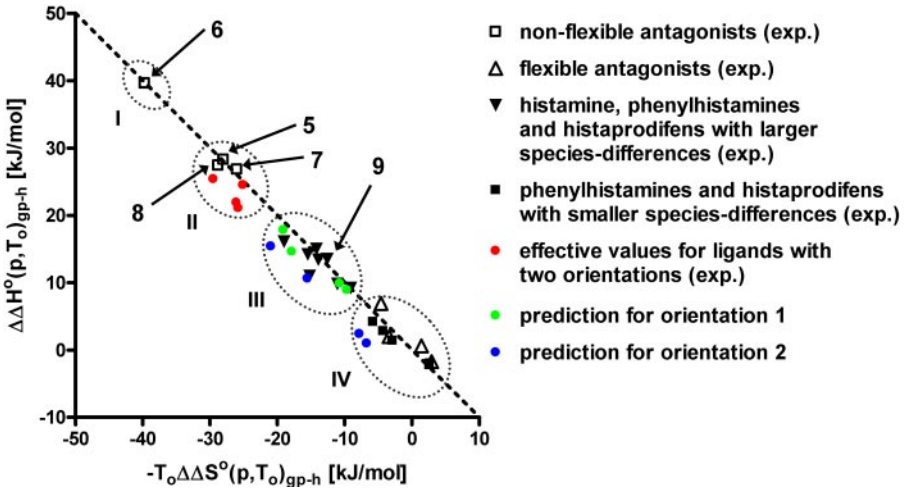

Fig. 9. Species differences in $\Delta H°(p,T_o)$ and $-T\Delta S°(p,T_o)$ between hH_1R and gpH_1R. The data points are calculated using the equations $\Delta\Delta H°(p,T_o)_{gp-h} = \Delta H°(p,T_o)_{gp} - \Delta H°(p,T_o)_h$ and $-T\Delta\Delta S°(p,T_o)_{gp-h} = -T\Delta S°(p,T_o)_{gp} + T\Delta S°(p,T_o)_h$ based on the data given in Table 2. Data points, exclusively based on experimental data are indicated by exp. The compounds are divided into the four groups in the following manner: I: black box, unfilled: **6**; II: black box, unfilled: **5**, **7**, **8**; red circle, filled: **19**, **20**, **21R**, **21S**; III: black triangle, filled: **9**, **10**, **12**, **13**, **15**, **16**, **17**, **22**; green circle, filled: **19**, **20**, **21R**, **21S**; blue circle, filled: **19**, **20**; IV: black triangle, unfilled: **1**, **2**, **3**, **4**; black box, filled: **11R**, **11S**, **14**, **18**; blue circle, filled: **21R**, **21S**.

approximately −600 to approximately 450 J/mol/K for GPCRs (Borea et al., 2000).

To our knowledge, we are the first to study the binding thermodynamics of the H_1-receptor, including H_1R antagonists and agonists with large structural differences. At 293.15 K, $\Delta H°(p,T_o)$ ranges from approximately −40 to approximately 90 kJ/mol, and $\Delta S°(p,T_o)$ ranges from approximately −20 to approximately 500 J/mol/K. These findings for the H_1R are in very good accordance with the findings for other GPCRs. The correlation between $\Delta H°(p,T_o)$ and $-T\Delta S°(p,T_o)$ for hH_1R and gpH_1R (Fig. 5) shows that discrimination between agonism and antagonism based on binding enthalpy and entropy is not possible for hH_1R and gpH_1R. Thus, the H_1R is more related to the D_2 and 5-HT_{1A} receptors than to β-adrenergic or adenosine receptors, concerning thermodynamic discrimination between agonism and antagonism. To obtain a more detailed insight in thermodynamic agonist-antagonist discrimination, even more compounds with high structural diversity have to be studied at several GPCRs.

For the process of ligand-binding to a receptor including receptor activation in case of agonists several subprocesses have to be considered: 1) Disruption of ligand-solvent-complex, 2) formation of ligand-receptor-complex, 3) conformational change of the ligand, 4) disruption of hydrogen-bonds in the receptor and formation of new hydrogen-bonds and, 5) change in receptor conformation. Thus, the energetic contribution of these subprocesses leads to the effective change in binding free energy, binding enthalpy, and binding entropy, which can be determined experimentally. Because of the complexity of this process, we propose that dependent on ligand structure but independent of agonistic or antagonistic function of the ligand, some of the subprocesses (i.e., 1 to 5) energetically cancel each other out or intensify each other. Thus, for a thermodynamic study of ligand-receptor interactions, a broad structural variety within the agonists and antagonists has to be guaranteed. Because changes in heat capacity for formation of ligand-receptor processes different from zero were observed, it should also be taken into account that an entropy-driven binding process can change to an enthalpy-driven binding process and vice versa with increasing temperature. Thus, the discrimination between agonism and antagonism may be a function of temperature.

Thermodynamic Measurements—A New Approach for the Dissection of Ligand-Specific Receptor Conformations? A number of experimental data based on fluorescence spectroscopy (Ghanouni et al., 2001) suggest the existence of agonist-dependent receptor conformations. Within the series of analyzed compounds in this study, our data suggest that the endogenous ligand histamine stabilizes the ligand-receptor-complex enthalpically, in contrast to the other analyzed agonists, where no enthalpic stabilization is observed (Fig. 5). Further studies including more natural or synthetic compounds have to be carried out to improve our knowledge about compounds being enthalpically favored in binding to the H_1R. One reason for the different behavior of histamine in contrast to phenylhistamines and histaprodifens concerning the enthalpy may be the different binding mode of histamine compared with those of phenylhistamines and histaprodifens (Fig. 8). It was shown experimentally that $Lys^{5.39}$ forms a hydrogen bond to the imidazole moiety of histamine (Jongejan and Leurs, 2005). In contrast, further experimental data show that an interaction between $Lys^{5.39}$ and histaprodifens is not established (Jongejan and Leurs, 2005). In addition, $Gln^{5.46}$ interacts with histamine but not with phenylhistamine (Leurs et al., 1994). If there is a compensation of the loss of enthalpy of solvation of histamine by a benefit of enthalpy of histamine-receptor interaction, the data suggest a receptor conformation specifically stabilized by histamine. In addition, it has to be considered that histamine, acting as full agonist, should promote a change of receptor conformation from inactive to active state. Thus, it may be speculated, that $\Delta H°(p,T_o)$ mainly includes the enthalpy related to changes in receptor conformation. These results are in good accordance with the description of agonist-dependent receptor conformations (Xie et al., 2006; Kobilka and Deupi, 2007).

The data (Fig. 9) suggest that the species differences in $\Delta\Delta H°(p,T_o)_{gp\text{-}h}$ and $\Delta\Delta S°(p,T_o)_{gp\text{-}h}$ are closely related to flexibility of the ligand and of the receptor. Antagonist **6** is very rigid and belongs to group I, which has the largest species differences. Antagonists **5**, **7**, and **8** belong to group II, which has smaller species differences, and have a rigid, tricyclic moiety, but there are flexible side chains. For the highly flexible antagonists **1** to **4**, belonging to group IV, no significant species differences are found. The flexible antagonists are able to undergo conformational changes to fit optimally into the binding pocket and to establish ligand-receptor interactions. Thus, these antagonists should be able to compensate for differences in receptor-flexibility between hH_1R and gpH_1R, which is not possible for the rigid antagonists. Because $\Delta H°(p,T_o)$ is significantly higher at gpH_1R than at hH_1R for the rigid antagonists, it can be supposed that hH_1R is more flexible than gpH_1R, resulting in a better ligand-receptor interaction at hH_1R. In addition, it should be considered, that it is proposed that antagonists do not induce a change of the receptor conformation from the inactive state to the active state. Thus, only the loss of enthalpy of solvation of the ligand and the benefit of ligand-receptor interactions should contribute to $\Delta H°(p,T_o)$. Because there are no differences in amino acids, interacting with antagonists in the binding pocket, between hH_1R and gpH_1R, there should be no differences in binding enthalpies between hH_1R and gpH_1R. This was observed for the flexible antagonists. Because of their flexibility, they can undergo conformational changes to fit optimally into the binding pocket of hH_1R and gpH_1R. Thus, there is no need for the receptor to change its conformation. In contrast, we observed species differences in binding enthalpy between hH_1R and gpH_1R in the range of approximately 25 to 40 kJ/mol for the rigid antagonists. Because there are no obvious differences in the binding pocket between hH_1R and gpH_1R, this result is surprising. Thus, these results may be explained by differences in flexibility of the receptor or compactness of the receptor structure caused by changes of H-bonding network of the receptor as a result of the differences in amino acid sequences between hH_1R and gpH_1R (Strasser et al., 2008b), especially concerning N terminus and E2-loop. Another possible explanation for the observed species differences of the rigid antagonists may be antagonist-dependent receptor conformations in the inactive state. Our data, based on thermodynamic measurements, suggest that different receptor conformations exist not only for the active state but also for the inactive state of the receptor. The species differences observed for the flexible

agonists may be explained in contrast to the antagonists, not with flexibility of the ligands but with species-dependent conformational changes of the receptor, because of its activation by the agonists. The division of the agonists in two groups (Fig. 9) may indicate that there exist agonist-dependent receptor conformations.

Conclusions

In our study, we have analyzed the binding of a large variety of antagonists and agonists to the hH_1R and gpH_1R thermodynamically. Our data suggest species differences between hH_1R and gpH_1R are observed not only in affinity but also in $\Delta H°(p,T)$ and $\Delta S°(p,T)$. In addition, our study shows that, in contrast to some other GPCRs, antagonists and agonists cannot be distinguished thermodynamically for the H_1R. But our data may suggest that there are different conformations not only of the active state of the receptor but also of the inactive state for the H_1R.

Acknowledgments

We thank G. Wilberg for competent help with the cell culture.

References

Borea PA, Varani K, Guerra L, Gilli P, and Gilli G (1992) Binding thermodynamics of A_1 adenosine receptor ligands. *Mol Neuropharmacol* **2:**273–281.

Borea PA, Dalpiaz A, Varani K, Gessi S, and Gilli G (1996) Binding thermodynamics at A_1 and A_{2A} adenosine receptors. *Life Sci* **59:**1373–1388.

Borea PA, Dalpiaz A, Varani K, Gilli P, and Gilli G (2000) Can thermodynamic measurements of receptor binding yield information on drug affinity and efficacy? *Biochem Pharmacol* **60:**1549–1556.

Bruysters M, Jongejan A, Gillard M, van de Manakker F, Bakker RA, Chatelain P, and Leurs R (2005) Pharmacological differences between human and guinea pig histamine H_1 receptors: Asn^{84} (2.61) as key residue within an additional binding pocket in the H_1 receptor. *Mol Pharmacol* **67:**1045–1052.

Casadó V, Allende G, Mallol J, Franco R, Lluis C, and Canela EI (1993) Thermodynamic analysis of agonist and antagonist binding to membrane-bound and solubilized A_1 adenosine receptors. *J Pharmacol Exp Ther* **266:**1463–1474.

Cheng Y and Prusoff WH (1973) Relationship between the inhibition constant (K1) and the concentration of inhibitor which causes 50 per cent inhibition (I50) of an enzymatic reaction. *Biochem Pharmacol* **22:**3099–3108.

Contreras ML, Wolfe BB, and Molinoff PB (1986) Thermodynamic properties of agonist interactions with the beta adrenergic receptor-coupled adenylate cyclase system. I. High- and low affinity states of agonist binding to membrane-bound beta-adrenergic receptors. *J Pharmacol Exp Ther* **237:**154–164.

Dalpiaz A, Borea PA, Gessi S, and Gilli G (1996) Binding thermodynamics of $5\text{-}HT_{1A}$ receptor ligands. *Eur J Pharmacol* **312:**107–114.

Duarte EP, Oliveira CR, and Carvalho AP (1988) Thermodynamic analysis of antagonist and agonist interactions with dopamine receptors. *Eur J Pharmacol* **147:**227–239.

Elz S, Kramer K, Pertz HH, Detert H, ter Laak AM, Kühne R, and Schunack W (2000) Histaprodifens: synthesis, pharmacological in vitro evaluation, and molecular modeling of a new class of highly active and selective histamine H_1-receptor agonists. *J Med Chem* **43:**1071–1084.

Ghanouni P, Steenhuis JJ, Farrens DL, and Kobilka BK (2001) Agonist-induced conformational changes in the G-protein-coupling domain of the β_2 adrenergic receptor. *Proc Natl Acad Sci U S A* **98:**5997–6002.

Harper EA and Black JW (2007a) Histamine H_3-receptor agonists and imidazole-based H_3-receptor antagonists can be thermodynamically discriminated. *Br J Pharmacol* **151:**504–517.

Harper EA, Roberts SP, and Kalindjian SB (2007b) Thermodynamic analysis of ligands at cholecystokinin CCK_2 receptors in rat cerebral cortex. *Br J Pharmacol* **151:**1352–1367.

Hill SJ, Ganellin CR, Timmerman H, Schwartz JC, Shankley NP, Young JM, Schunack W, Levi R, and Haas HL (1997) International Union of Pharmacology. XIII. Classification of histamine receptors. *Pharmacol Rev* **49:**253–278.

Jongejan A and Leurs R (2005) Delineation of receptor-ligand interactions at the human histamine H_1 receptor by a combined approach of site-directed mutagenesis and computational techniques—or—how to bind the H_1 receptor. *Arch Pharm (Weinheim)* **328:**248–259.

Kelley MT, Bürckstümmer T, Wenzel-Seifert K, Dove S, Buschauer A, and Seifert R (2001) Distinct interaction of human and guinea pig histamine H_2-receptor with guanidine-type agonists. *Mol Pharmacol* **60:**1210–1225.

Kilpatrick GJ, el Tayar N, Van de Waterbeemd H, Jenner P, Testa B, and Marsden CD (1986) The thermodynamics of agonist and antagonist binding to dopamine D-2 receptors. *Mol Pharmacol* **30:**226–234.

Kobilka BK and Deupi X (2007) Conformational complexity of G-protein-coupled receptors. *Trends Pharmacol Sci* **28:**397–406.

Leschke C, Elz S, Garbarg M, and Schunack W (1995) Synthesis and histamine H_1 receptor agonist activity of a series of 2-phenylhistamines, 2-heteroarylhistamines, and analogues. *J Med Chem* **38:**1287–1294.

Leurs R, Smit MJ, Tensen CP, Ter Laak AM, and Timmerman H (1994) Site-directed mutagenesis of the histamine H_1-receptor reveals a selective interaction of asparagine207 with subclasses of H_1-receptor agonists. *Biochem Biophys Res Commun* **201:**295–301.

Menghin S, Pertz HH, Kramer K, Seifert R, Schunack W, and Elz S (2003) N_α-Imidazolylalkyl and pyridylalkyl derivatives of histaprodifen: synthesis and in vitro evaluation of highly potent histamine H_1-receptor agonists. *J Med Chem* **46:**5458–5470.

Menghin S (2004) Analoge des Histaprodifens als potente und selektive Agonisten des Histamin-H_1-Rezeptors. Ph.D. dissertation, Free University of Berlin, Berlin, Germany.

Seifert R, Wenzel-Seifert K, Burckstummer T, Pertz HH, Schunack W, Dove S, Buschauer A, and Elz S (2003) Multiple differences in agonist and antagonist pharmacology between human and guinea pig histamine H_1-receptor. *J Pharmacol Exp Ther* **305:**1104–1115.

Strasser A, Striegl B, Wittmann HJ, and Seifert R (2008a) Pharmacological profile of histaprodifens at four recombinant histamine H_1 receptor species isoforms. *J Pharmacol Exp Ther* **324:**60–71.

Strasser A, Wittmann HJ, and Seifert R (2008b) Ligand-specific contribution of the N terminus and E2-loop to pharmacological properties of the histamine H_1-receptor. *J Pharmacol Exp Ther* **326:**783–791.

Strasser A, Wittmann HJ, Kunze M, Elz S, and Seifert R (2009) Molecular basis for the selective interaction of synthetic agonists with the human histamine H_1-receptor compared with the guinea pig H_1-receptor. *Mol Pharmacol* **75:**454–465.

Weiland GA, Minneman KP, and Molinoff PB (1979) Fundamental difference between the molecular interactions of agonists and antagonists with the β-adrenergic receptor. *Nature* **281:**114–117.

Wieland K, Laak AM, Smit MJ, Kühne R, Timmerman H, and Leurs R (1999) Mutational analysis of the antagonist-binding site of the histamine H_1 receptor. *J Biol Chem* **274:**29994–30000.

Williams DH, O'Brien DP, Sandercock AM, and Stephens E (2004) Order changes within receptor systems upon ligand binding: receptor tightening/oligomerisation and the interpretation of binding parameters. *J Mol Biol* **340:**37–383.

Wold S, Johansson A, and Cochi M (1993) PLS—partial least squares projection to latent structures, in *3D QSAR in Drug Design: Theory, Methods and Applications* (Kubinyi H ed), p 523–550, ESCOM, Leiden.

Xie SX, Ghorai P, Ye QZ, Buschauer A, and Seifert R (2006) Probing ligand-specific histamine H_1- and H_2-receptor conformations with N^G-acylated imidazolylpropylguanidines. *J Pharmacol Exp Ther* **317:**139–146.

Zingel V, Leschke C, and Schunack W (1995) Developments in histamine H_1-receptor agonists. *Prog Drug Res* **44:**49–85.

Address correspondence to: Dr. Andrea Strasser, Department of Pharmaceutical and Medicinal Chemistry I, University of Regensburg, Universitätsstraße 31, D-93053 Regensburg, Germany. E-mail: andrea.strasser@chemie.uni-regensburg.de